

# Transient trapping of two microparticles interacting with optical tweezers and cavitation bubbles

Viridiana Carmona-Sosa<sup>1</sup> and Pedro A. Quinto-Su<sup>1,\*</sup>

<sup>1</sup>*Instituto de Ciencias Nucleares, Universidad Nacional Autónoma de México  
Apartado Postal 70-543, 04510, México D.F., México.*

In this work we show that two absorbing microbeads can briefly share the same optical trap. Optical forces pull the particles towards the waist of the trapping beam. However, once a particle reaches the vicinity of the waist, the surrounding liquid is superheated creating an explosion or cavitation bubble that pushes the particle away while lengthening or shortening the trajectories of the surrounding particles. In this way each particle briefly interacts with the beam waist at different times. We find that when two microbeads reach the waist simultaneously, a larger explosion might result in ejection from the trap. We measure the characteristic timescale of two particle coalescence near the waist and find a Poisson decaying exponential probability distribution. The results are consistent with a simple simulation and show why the characteristic timescales for transient trapping of multiple absorbing particles decrease as more objects are added.

## I. INTRODUCTION

Highly focused continuous laser beams or optical tweezers have been used to trap microscopic objects that are held by forces that are proportional to the gradient of the intensity [1]. Observations have shown that multiple particles can be trapped with single optical tweezers [2].

A single focused laser spot can also trap multiple particles at different spatial locations by periodically steering the beam so that the trap is shared [3–5]. This technique has also been applied for directed diffusion of multiple beads or optical peristalsis [6]. Other transient trapping regimes periodically block the trapping beam with an optical chopper to study free diffusion while not allowing the particles to drift outside the imaging area. This has been called blinking optical tweezers [7].

Partially absorbing particles can interact briefly with the beam waist of an optical trap in a cyclic way under the effect of optical forces and microexplosions or cavitation bubbles [8]. A bead that is located below the waist of the trapping beam is pulled by gradient forces to the focused spot. However, as the particle approaches the waist the heating rate increases until a small volume of the surrounding liquid is superheated creating a cavitation bubble that expands and collapses in a microsecond timescale. The bubble pushes the particle below the waist where the cycle restarts. Hence the particle is essentially always moving in the direction of the focused spot (millisecond timescale) while the motion due to the explosion lasts about a few microseconds.

Here we show that a system of two absorbing microbeads can share a static optical trap at different times. Each time a particle reaches the waist creating an explosion, the individual cycles of the neighboring particles towards the waist are shortened or lengthened depending on the size of the bubble and the distance to the waist.

We find that the particles can coexist in the neighborhood of the trap as long as they do not approach the waist simultaneously, which may result in a larger bubble that can eject the particles. The characteristic lifetime of the particles in the trap is defined in terms of the time intervals between events of particle coalescence at the waist. The distribution of these measured intervals lie in an decaying exponential. The experimental results are confirmed with a simple one dimensional Langevin simulation coupled to an empirical model for the bubble size distribution and the interaction between bubble and particle [9, 10].

## II. EXPERIMENT

The experiments are done in a near IR optical tweezers setup described in [8, 10]. The trapping laser wavelength is 975 nm and it is focused by a  $100\times/1.25$  NA microscope objective with a transmitted power of 62 mW. The microparticles are magnetic beads (Promag Bangs) with a mean diameter of  $3.16\ \mu\text{m}$  immersed in water. The aqueous sample is placed between two microscope coverslips with a separation  $\sim 100\ \mu\text{m}$ . The dynamics are captured with high speed video recorder at 2,000 and 300,000 frames per second (fps). The slower recording speed is used to capture the overall dynamics for a few seconds while the higher speed can capture the explosions in a single frame to measure the maximum sizes of the cavitation bubbles.

The trapping beam waist is raised above the bottom coverslip at a height of between 15 and  $25\ \mu\text{m}$ . Initially, the particles are near the bottom and within a few micrometers (radial) from the center of the beam waist. The particles are pulled to the waist and later are pushed away by the explosion, the total displacement and direction are random as these depend on the size of the bubble and the location where the bubble is created. Typical displacements are on the order of  $10\ \mu\text{m}$  in the axial  $z$  direction and a few microns in the transverse plane  $xy$

---

\*E-mail: pedro.quinto@nucleares.unam.mx

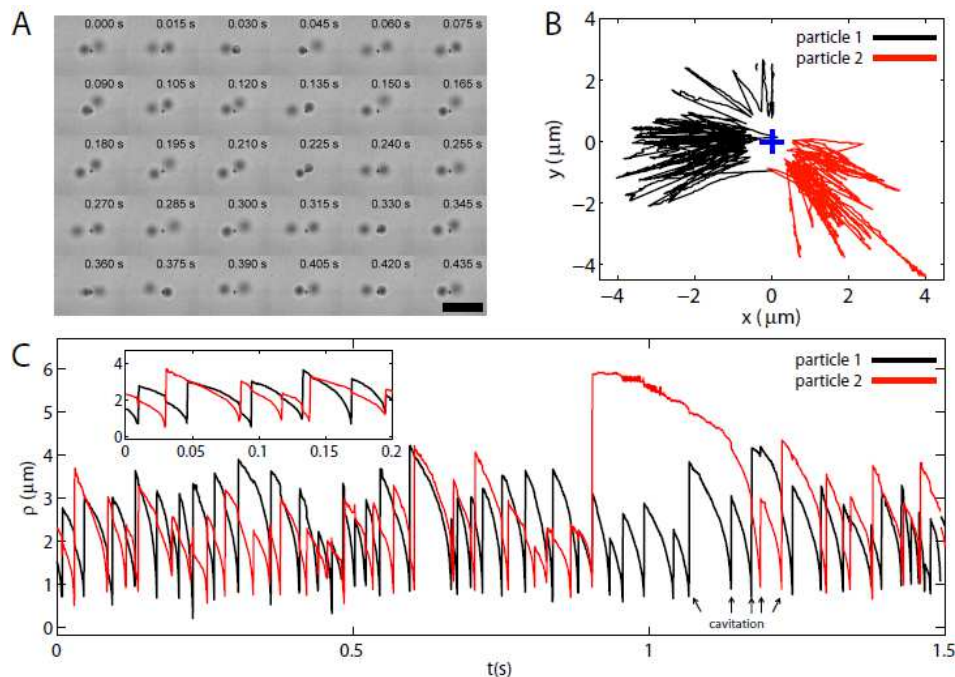


FIG. 1: Two particle interaction. (A) Extracted frames from Visualization 1. The time step between each frame is 0.015 s for a total of 0.435 s. The size of each frame is  $18 \times 15 \mu\text{m}$ . The scale bar has a width of  $10 \mu\text{m}$ . (B) Trajectories of the particles in (A) for a time of 1.5 s. The cross marks the position of the trap center. (c) Dynamics for  $\rho(t)$  (radial distance from the center of the trap at the  $xy$  plane) for both particles. During each cavitation event there is an effect (push, pull, neutral) on the trajectory of the neighboring particle (inset).

which is the one that we image [8].

### III. RESULTS AND DISCUSSION

In Figure 1A we show selected frames from Visualization 1, recorded at 2,000 fps. The particles appear blurred when the axial position is below the waist of the trapping beam. As the particles get closer to the beam waist they appear sharper.

From the visualizations we extract the two dimensional position of the particles. The extracted trajectories  $(x(t) - x_0, y(t) - y_0)$  are plotted in Fig. 1B, where  $(x_0, y_0)$  are the coordinates of the trap center (marked with a cross). We observe that as the particles climb towards the trapping beam waist, the distance  $\rho(t) = \sqrt{(x(t) - x_0)^2 + (y(t) - y_0)^2}$  in the  $xy$  plane to the center of the trap also decreases. Figure 1C shows the dynamics  $\rho(t)$  of each particle. The cavitation events are the sharp transitions with relatively large displacements in a single time step. In the inset of Fig. 1C we observe that during each cavitation event initiated by the particle nearest to the waist, the neighboring particle is also affected. These interactions are similar to those of oscillators that are synchronized through pulses [11]. However, pulse synchronization seems to have little effect since both the size of each bubble and the period of each cycle are random.

The total displacement on a particle  $\Delta x'$  due to a cavitation event depends on the distance  $\delta'$  from the center of the particle to the origin of the bubble, the maximum bubble radius  $R_{max}$  and the particle radius  $R$ . The interaction is described by the mastercurve shown in Fig. 2A [9], where  $\Delta x = \Delta x'/(2R)$  and  $\delta = \delta'/R_{max}$ . A particle can be pushed ( $\Delta x > 0$ ) when  $\delta < 0.7$ , pulled ( $\Delta x < 0$ ) when  $0.7 < \delta_i < 3.7$  or leave the particle in the same position ( $\Delta x = 0$ ) when  $\delta = 0.7$ . In the case of one particle the interaction is in the regime of rejection or pushing  $\delta < 0.7$ .

Figure 2B (top) shows how a bubble is created at the surface of a particle that approaches the waist of the trapping beam, in that case the top surface is the one where higher temperatures are reached (red dot) and as a result a small volume of liquid in contact with that surface is superheated creating a cavitation bubble. Hence the distance from the origin of the bubble to the center of the particle  $\delta'$  is the radius of the particle  $R$ . When two particles are sharing the trap (Fig. 2B bottom), each cavitation event results in a net displacement  $\Delta x'_i$  for both particles, the particle that creates the bubble is pushed while the displacement of the neighboring particle depends on the value of  $\delta'_i$  (distance to the origin of the bubble at the surface of the other particle). However the effect on the second particle also depends on the direction in which the first particle is pushed which creates an asymmetry in the flow [8]. Hence the mastercurve only

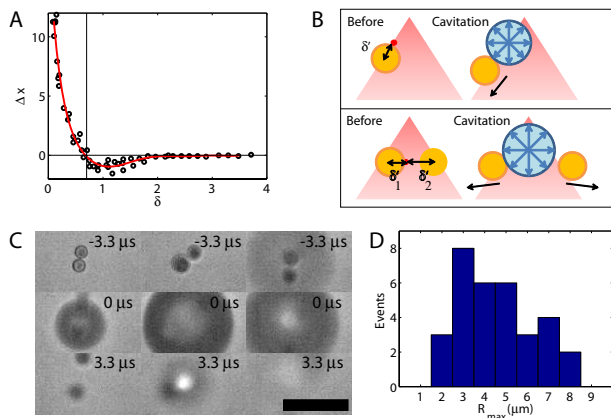


FIG. 2: (A) Mastercurve for the interaction between particle and bubble.  $\delta = \delta'/R_{max}$ ,  $\Delta x = \Delta x'/(2R)$ . (B) Bubble particle interaction. Top: single particle. Bottom: two particles reaching the waist simultaneously. (C) Frames extracted from recordings at 300,000 fps. Each column is for different events. The width of the scale bar is 10  $\mu\text{m}$ . (D) Histograms for measured bubbles when the particle separation of less than 3.6  $\mu\text{m}$  prior to cavitation.

provides a qualitative description for the neighboring objects.

We observe that the particles are usually ejected from the trap when both approach the waist of the trapping beam simultaneously, when the radial distance to the center of the waist for both particles prior to cavitation is less than  $\rho_0 = 1.8 \mu\text{m}$ . In many of these events we find a significant larger lateral displacement ( $xy$  plane) for at least one of the particles of about  $\sim 6 \mu\text{m}$ . The large displacements could be explained by larger bubbles and by the location where the bubbles are produced. When both particles approach the waist simultaneously, there is the possibility of reaching higher temperatures between the particles (Fig. 2B, bottom) rather than at the top, creating a bubble at the surface of one particle that will push both objects predominantly in the transverse direction. In contrast to the case depicted in Fig. 2B (top) where the displacement of a particle is larger in the axial direction with small components in the transverse direction.

When a particle is pushed far away from the center of the trap where essentially there is no interaction with the optical tweezers, it is possible that the particle will be attracted back to the trap by another particle that is oscillating in the trap.

To measure the maximum bubble sizes  $R_{max}$  we record the interaction between particles at 300,000 fps. Selected frames from three different events are shown in Fig. 2C, where the frames correspond 3.3  $\mu\text{s}$  before cavitation, during cavitation and 3.3  $\mu\text{s}$  after the explosion. The size distribution  $R_{max}$  for the bubbles measured when the separation between the particles is less than 3.6  $\mu\text{m}$  prior to the explosion is in Fig. 2D. 36% of the bubbles

have a size between 5 and 8  $\mu\text{m}$ , which is significantly larger than the distribution measured for single particles where only 6% of the bubbles are larger than 6  $\mu\text{m}$  [10].

These measurements suggest that when both particles are near the waist higher superheat temperatures are reached or larger volumes of liquid are superheated, which should result in higher pressures and a larger bubble originating at the surface of one of the particles [8]. Furthermore, the push can have a larger component in the transverse direction as shown in Fig. 2B (bottom).

In order to characterize the typical times where we would expect to have both particles oscillating in the vicinity of the trap ( $\rho < 4.5 \mu\text{m}$ ) we define a characteristic time as the time interval  $\Delta t$  between events where both particles coalesce at the waist (within 1.8  $\mu\text{m}$ ) and are more likely to be ejected or pushed away from the interaction region of the trap. We can measure these intervals from the trajectories like that shown in Fig. 1C. In our experiments we measure 1779 individual cycles and find 130 events where the particles reach the center simultaneously.

The distribution for the measured  $\Delta t$  (between particle coalescence) is shown in Fig. 3A and corresponds to a Poisson process that implies an exponential decay. The continuous line is  $\propto \exp(-\Delta t/\mu)$ , where  $\mu = 0.18 \text{ s}$ . The distribution suggests that the characteristic particle coalescence times can be described assuming that the events are independent and with no memory, that  $\Delta t$  depends on the random individual cycle frequencies. The distribution is consistent with the measurements that show that at each cavitation event there is a perturbation in the neighboring particle (attractive, repulsive or neutral displacement) which essentially resets the system, erasing the previous trajectory. Figure 3B shows a distribution for  $\Delta t$  extracted from simulated trajectories (Fig. 3C), where  $\mu = 0.2 \text{ s}$ . The simulation is described in the following paragraphs.

#### IV. SIMULATION

We simulate the particle dynamics with a one dimensional Langevin equation [12] for the axial direction in order to simplify the system by removing the random direction in which a particle is pushed during cavitation and the asymmetry created by the particle displacement. Besides, the displacements are larger in the axial direction while there is no particle coalescence and the gradient force is weaker limiting the individual period or return time to the beam waist of each particle.

$$m\ddot{z} = F(z) - \gamma\dot{z} + \sqrt{2k_B T \gamma} W(t) \quad (1)$$

where  $m$  is the effective mass of the particle  $\rho_p V_p + \rho_l V_p/2$ , with  $V_p = 4\pi R^3/3$  the particle volume,  $R$  the radius,  $\rho_p$  the particle density and  $\rho_l$  the liquid density.  $\gamma = 6\pi\eta R$  is the Stokes drag with  $\eta = 0.001 \text{ Ns/m}^2$ . The diffusion coefficient is  $D = k_B T/\gamma$  with  $k_B$  the Boltzmann constant,  $T = 300\text{K}$  the room temperature and  $W(t)$  is the white

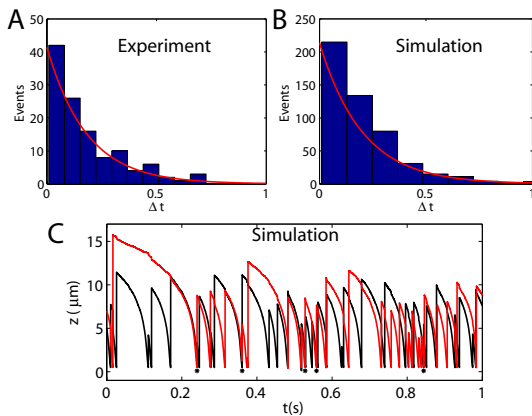


FIG. 3: (A) Measured distribution for  $\Delta t$  (interval between coalescence events) with fitted exponential  $\propto \exp(-\Delta t/\mu)$ , with  $\mu = 0.18$  s. (B) Distribution for  $\Delta t$  extracted from simulated trajectories.  $\mu = 0.2$  s. (C) Simulated trajectories (in  $z$ ) of two particles and their interaction during cavitation.

noise [12]. The force  $F(z)$  is proportional to the axial gradient of a Gaussian beam  $F(z) = A_0 z_R^2 z / (z_R^2 + z^2)^2$ . The parameters  $A_0$  and the Rayleigh range  $z_R$  are chosen to mimic the measured individual cycle frequencies as a function of the maximum displacements that are correlated with  $R_{max}$ . We use  $z_R = 3.5 \times 10^{-6}$  m and  $I_0 = 1.8 \times 10^{-16}$  J. We use the Euler method to solve for  $z(t)$  with a time step  $dt = 10^{-4}$  s. In this limit if we divide [Eq. (1)] by  $\gamma$ , the factor  $(m/\gamma)$  can be neglected. Hence the non-inertial approximation is

$$\dot{z} = F(z)/\gamma + \sqrt{\frac{2k_B T}{\gamma}} W(t) \quad (2)$$

The initial condition at  $t = 0$  s is  $z(0) = z_0$  and with zero initial velocity  $\dot{z}(0) = 0$   $\mu\text{m/s}$ .

In order to simulate cavitation we impose the condition that when  $z$  reaches a value  $z < 0.5$   $\mu\text{m}$  (at time  $t_0$ ) then a bubble with a maximum size  $R_{max}$  is created. The size is chosen randomly from a Gaussian size distribution centered at 3.9  $\mu\text{m}$  and with a standard deviation of 0.6  $\mu\text{m}$  in order to limit size of the bubbles between 2 and 6  $\mu\text{m}$  [10]. After choosing  $R_{max}$  the new position  $z(t_0) = z_0 = \Delta x(\delta)$  of the particle is calculated from the interpolated data [9] in Fig. 2A (red line). The speed is set at  $\dot{z}(t_0) = 0$   $\mu\text{m/s}$  and the simulation restarts with those new initial conditions.

In the case of two particles that only interact during the cavitation events we added the condition that during cavitation at  $t_0$  the distance to the other particle is measured  $\Delta z = |z_2(t_0) - z_1(t_0)|$  in order to also calculate the induced displacement (positive, negative or neutral) on that particle. In this way after cavitation (assuming generated by particle 1):  $z_1(t_0) = z_{10} = \Delta x_1(\delta_1)$ ,  $\dot{z}_1(t_0) = 0$   $\mu\text{m/s}$ ,  $z_2(t_0) = z_2(t_0 - dt) + \Delta x_2(\delta_2)(2R)$ ,  $\dot{z}_2(t_0) = 0$   $\mu\text{m/s}$  with  $\delta_1 = R/R_{max}$  and  $\delta_2 = (\Delta z +$

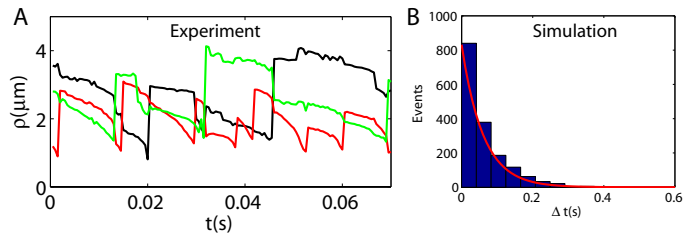


FIG. 4: Three particles oscillating in an optical tweezers. (A) Dynamics  $\rho_i(t)$  extracted from Visualization 2. (B) Two-particle coalescence time  $\Delta t$  extracted from simulations with three particles,  $\mu = 0.06$  s.

$R)/R_{max}$ . A few cycles are shown in Fig. 3C. Notice that the axial displacements on the order of 10  $\mu\text{m}$  are larger than the measured radial displacements in Fig. 1C as expected [8].

A sample of the simulated particle dynamics are shown in Fig. 3C. The dynamics are calculated for a million timesteps and the time intervals between coalescence at  $\Delta z < 1.8$   $\mu\text{m}$  are extracted just like in the experimental measurements. The simulation has 5424 cavitation events with particle coalescence at 496. The histogram extracted from the simulations is shown in Fig. 3B, with an exponential fit with  $\mu = 0.2$  s which agrees with our measurements.

**Three particles.** In our experiments it was difficult to observe three or more particles oscillating within  $\rho \sim 4.5$   $\mu\text{m}$  from the center of the trap, since in a very short time a pair of particles reach the waist simultaneously ejecting at least one particle from the trap (to a radial distance  $\sim 6$   $\mu\text{m}$ ). In this way experiments on the interaction between three particles most of the time are reduced to the interaction between two particles. The presence of an extra particle accelerates the characteristic time for coalescence of a pair  $\Delta t$  and typically resulted in the ejection of a single particle at a distance  $\rho \sim 6$   $\mu\text{m}$ . Hence we only recorded few cycles when three particles were oscillating close to the trap.

Figure 4A shows the dynamics of three particles extracted from Visualization 2. The characteristic times for coalescence of a pair are shown in Fig. 4B and are extracted from a simulation of three particles with 8222 cavitation events with particle pair coalescence at 1649. The distribution with  $\mu = 0.06$  s (red continuous line) shows that the typical timescales are drastically reduced, which explains the shorter time intervals where three particles may oscillate in the vicinity of a single optical tweezers.

## V. CONCLUSION

We have shown that two particles can coexist in an optical trap by sharing the beam waist at different times and that the particles may be ejected when reaching the

waist simultaneously due to larger bubbles that result from higher temperatures or a larger superheated volume of liquid. The Poisson distribution shows that the system can be modeled as independent random oscillators. This is consistent with the observations of the system resetting at each cavitation event.

As more particles are added, other thermal effects that were neglected like convection and thermophoresis [13] should become more important.

### Supplementary Material

. Visualization 1. Two particles, recording at 2,000 fps, slowed 100 times. 1 second displayed in 100 s at 20

fps. Frame size:  $18 \times 15 \mu\text{m}$ .

Visualization 2. Three particles, recording at 2,000 fps, slowed 100 times. 0.5 second displayed in 50 s at 20 fps. Frame size  $18 \times 15 \mu\text{m}$ .

### Acknowledgments

Work partially funded by DGAPA-UNAM project IN104415.

- 
- [1] J.E. Molloy, and M.J. Padgett, *Contemp. Phys.*, **43**, 241 (2002).
  - [2] M. Li, and J. Arlt, *Opt. Commun.*, **281**, 135 (2008).
  - [3] M. Capitanio, R. Cicchi, and F.S. Pavone, *Opt. Laser Eng.*, **45**, 450 (2007).
  - [4] Y. Tanaka, *J. Opt.*, **15**, 025708 (2013).
  - [5] L. Yu, and Y. Sheng, *Opt. Express*, **22**, 7953 (2014).
  - [6] B.A. Koss, and D.G. Grier, *Appl. Phys. Lett.*, **82**, 3985 (2003).
  - [7] J.C. Crocker, and D.G. Grier, *J. Colloid Interface Sci.*, **179**, 298 (1996).
  - [8] P.A. Quinto-Su, *Nat. Commun.*, **5**, 5889 (2014).
  - [9] S.R. Gonzalez-Avila, X.H. Huang, P. A. Quinto-Su, T. Wu, and C.D. Ohl, *Phys. Rev. Lett.* **107**, 074503 (2011).
  - [10] V. Carmona-Sosa, J.E. Alba-Arroyo and P.A. Quinto-Su, arXiv: 1507.06255v1.
  - [11] R.E. Mirollo, and S.H. Strogatz, *SIAM J. Appl. Math.*, **50**, 1645 (1990).
  - [12] G. Volpe and G. Volpe, *Am. J. Phys.*, **81**, 224 (2013).
  - [13] S. Duhr, and D. Braun, *PNAS*, **103**, 19678 (2006).